



Influence of Multi-Axial Isothermal Forging on the Stability of Martensitic Transformation in a Heusler Ni-Mn-Ga Alloy

I. I. Musabirov¹  · I. M. Safarov¹ · R. M. Galejev¹ · D. D. Afonichev¹ · R. Y. Gaifullin² · V. S. Kalashnikov³ · E. T. Dilmieva³ · V. V. Koledov³ · S. V. Taskaev^{4,5} · R. R. Mulyukov¹

Received: 5 May 2021 / Accepted: 24 June 2021 / Published online: 16 July 2021
© The Indian Institute of Metals - IIM 2021

Abstract The Heusler alloys demonstrate magnetically induced strain and magnetocaloric properties, but the mechanical properties are poor. Therefore, in this work, the influence of thermomechanical treatment on the properties of Ni-Mn-Ga-Si Heusler alloys is considered. The effect of multi-axial isothermal forging on functional properties of the Ni_{2.30}Mn_{0.73}Ga_{0.90}Si_{0.07} alloy at 973 K and true strain (ϵ) of 3.9 is presented. It is shown that a unique two-phase microstructure is formed as a result of forging. The large grains in the size range of 100–200 μm are surrounded by a fine-grained structure. The study of the thermomechanical properties by the three-point bend test has shown that the alloy demonstrates a single-stage reversible deformation of 3.1% at a constant stress of 860 MPa as compared to the same alloy in the as-cast condition which shows 2% at 380 MPa. The specimen demonstrates a reversible deformation of 5% without any degradation during thermal cycling (with a base of up to 4000 thermal cycles) under a stress of 550 MPa and up to 5% with degradation occurring at 700 thermal cycles under a stress of 650 MPa. Thus, forging makes it possible to obtain a material with higher operational properties and greater resistance to fracture during multiple cycles of martensitic transformation. In this

case, it is possible to obtain anisotropy of properties equal or close to that of the specimen in the as-cast state.

Keywords Heusler alloy · Ni–Mn–Ga · Martensitic transformation · Multi-axial isothermal forging · The shape memory effect · Anisotropy

1 Introduction

Heusler alloys undergoing martensitic transformation demonstrate the presence of such unique properties as the ferromagnetic shape memory effect, magnetocaloric effect, etc. The ferromagnetic shape memory effect caused by the reorientation of the martensitic structure has an irreversible deformation of about 12% for a single-crystal specimen [1–3]. In the polycrystalline state, this value varies from 0.16% to 1% [4, 5]. For example, in [4] it was shown that the value of reversible magnetically induced strain of 0.2% was achieved due to the orientation of internal stresses by subjecting the alloy to superplastic training. In [5], the preliminary training of the Ni₅₀Mn₂₉Ga₂₁ alloy made it possible to obtain an even greater magnitude of magnetically induced strain, which reached a value of 1% at a magnetic field strength of ~ 1 T. The authors explained it in terms of internal stresses, which led to the preferred orientation of martensite. Also, a greater magnitude of magnetically induced strain was demonstrated in [6]. In the Ni₂Mn_{0.7}Cu_{0.3}Ga_{0.84}Al_{0.16} alloy, the irreversible deformation of up to 2% is shown at a magnetic field strength of ~ 1 T. This high magnetically induced strain is explained by the abrupt (practically isothermal) occurrence of the martensitic transformation. However, as is discussed in the work, a specimen with about 2 mm size was selected

✉ I. I. Musabirov
irekmusabirov@mail.ru

¹ Institute for Metals Superplasticity Problems of RAS, Ufa 450001, Russia

² Bashkir State University, Ufa 450076, Russia

³ Kotelnikov Institute of Radioengineering and Electronics of RAS, Moscow 125009, Russia

⁴ Chelyabinsk State University, Chelyabinsk 454001, Russia

⁵ South Ural State University, Chelyabinsk 454080, Russia

for the studies. Such a specimen might not quite relate to polycrystalline materials, since during argon-arc melting of the alloy, elongated crystals of about 1 mm length and 0.5 mm diameter were formed in the structure. Thus, it can be concluded that the preferred orientation of internal stresses contributes to the formation of a preferred orientation of martensite, which ensures a higher magnitude of magnetically induced strain.

Despite the reduced magnitude of the effect on polycrystals as compared to single crystals, it is sufficient to consider these materials as appropriate for magnetically controlled devices. For monocrystalline and polycrystalline specimens, a general disadvantage is reduced mechanical properties [7]. At multiple cycles of martensitic transformation, the functional effect decreases and the specimen can be fractured [8]. Usually, in order to obtain a material with improved properties, it is subjected to various types of thermomechanical treatment (TMT). In the case of Heusler alloys, methods involving large plastic deformations, such as high-pressure torsion [9–12], rolling [13], upsetting (forging) [14] or extrusion [15–19], are used. In most cases, it leads to a decrease in the functional characteristics. The presence of dislocations plays a positive role, since they are sources of martensite growth during repeated cycles of phase transformation. TMT of the alloy, for example extrusion, significantly increases the mechanical properties. It was shown in [20] that thermal treatment at 1323 K of the $\text{Ni}_{50.4}\text{Mn}_{27.3}\text{Ga}_{22.3}$ alloy led to the formation of a sharp texture, which in turn contributed to the formation of a preferred martensite plate orientation during the phase transformation. Such a specimen can withstand up to 250 cycles without degradation of the elastocaloric effect.

The schemes and modes of thermomechanical treatment by multi-axial isothermal forging (MIF) and forging followed by extrusion have been intensively developed by the authors, and their influence on the functional properties of Ni-Mn-Ga system Heusler alloys has been studied [14, 17–19]. The advantage of this treatment is the production of a bulk material with the required microstructure and different levels of micro-stresses and texture. In the final stages of deformation processing (so-called drawing), the formation of a sharp crystallographic texture is possible, which is an important aspect for obtaining the maximum possible value of the functional effect. After forging of the alloy, a working element of the required shape and size can be cut from the sample obtained. Preliminary experiments show that as a result of forging at 973 K and a true strain (ϵ) of 1.9, a two-phase grain structure is formed [14]. The abrupt change of the geometric dimensions (anisotropy) of thermally treated state is shown by the analysis of the thermal expansion in the martensitic transformation range. The anisotropy level is close to that in the as-cast state. This means that the MIF does not lead to the

degradation of the functional characteristics and that a significant magnitude of the ferromagnetic shape memory effect can be obtained in such a specimen.

This work presents the effect of thermomechanical treatment using the multi-axial isothermal forging at a temperature of 973 K and the true strain (ϵ) of 3.9 on the microstructure, physical and mechanical properties of the $\text{Ni}_{2.30}\text{Mn}_{0.73}\text{Ga}_{0.90}\text{Si}_{0.07}$ Heusler alloy.

2 Experimental Procedure

A $\text{Ni}_{2.30}\text{Mn}_{0.73}\text{Ga}_{0.90}\text{Si}_{0.07}$ alloy was synthesized by argon-arc melting from elements of high purity. Usually the ingots, melted by this method, have the shape of “tablets.” Melting was done using a water-cooled copper base. As a result, intense cooling of the ingot and high-speed of crystallization occurred. Large elongated grains were formed. Such crystals have a non-uniform grain boundary. At temperatures close to or below the martensitic transformation thermal hysteresis interval, the additional internal stresses were created giving rise to the phase transformation. Such a microstructure is not suitable for thermomechanical treatment, since fracture of the specimen is possible along non-uniform boundaries. To eliminate the above imperfections in the structure, the ingot was subjected to additional vacuum induction remelting (VIR) in a quartz crucible. As a result of slow crystallization, a homogeneous microstructure with equiaxed grains was formed. Thus, in this paper, the as-cast state corresponds to an alloy synthesized by argon-arc melting with subsequent VIR.

The chemical composition of the alloy was analyzed by energy-dispersive spectroscopy using an X-Act attachment (Oxford Instruments) installed on a Vega 3 SBH scanning electron microscope (Tescan). It is confirmed by the chemical composition analyses of the alloy that it corresponds to $\text{Ni}_{2.30}\text{Mn}_{0.73}\text{Ga}_{0.90}\text{Si}_{0.07}$. The presence of silicon is explained by its diffusion from the crucible during VIR. Its distribution through the volume is uniform. The localization in the form of particles and phases is absent. After removal of the shrinkage cavity of the cylindrical sample, it was subjected to thermomechanical treatment by the multi-axial isothermal forging. The cylindrical sample before forging had a diameter of 16.8 mm and a height of 22.3 mm. A schematic of the mechanical working of the sample is shown in Fig. 1a.

The alloy was mechanically worked on a Schenck Trebel RMC 100 complex loading machine. Staged upsetting of the sample by 35–40% was done at a temperature of 973 K and a strain rate of 0.2 mm/min. The mechanical working compressed the 9 stages of upsetting in the following sequence: OZ → OY → OX → OY →

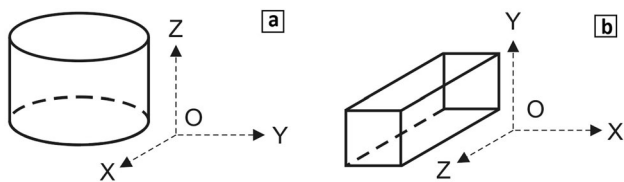


Fig. 1 Scheme of directions of the sample in the as-cast state (a) and after multi-axial isothermal forging at 973 K (b)

OX → OY → OX → OY → OX. In the final 6 stages (drawing), the sample was upset along only two axes to form the required texture. A total true strain (ϵ) of 3.9 was achieved. As a result of forging, the sample was obtained in the shape of an elongated parallelepiped with sides of 15.5 mm × 10.8 mm × 30.3 mm. The OZ axis is the drawing axis, while OY is coaxial to the final upset (Fig. 1b).

The microstructure was investigated using a high-resolution scanning electron microscope Mira3 LMH (Tescan) in the BSE mode at room temperature. The specimens were prepared by electropolishing in an electrolyte with 90% n-butyl alcohol (C₄H₉OH) and 10% HCl. The magnetic properties of the alloy were measured on a Lake Shore 7407 vibration magnetometer (Cryotronics) on specimens with 2 mm × 2 mm × 1 mm size with the magnetic field ranging up to 30 kOe. The $M(T)$ curves were recorded in the range from room temperature to 573 K. The characteristic martensitic transformation temperatures were determined by differential scanning calorimetry on a Jupiter STA 449 F1 (Netzsch) installation. The heating/cooling rate of the specimen was 1 K/min during measurements. The analysis of the anisotropy of thermal expansion was carried out using a dilatometer designed and fabricated in-house. The measurements were carried out on specimens with 1 mm × 1 mm × 7 mm size along the long side in the temperature range from 373 to 533 K. The thermomechanical properties were evaluated by three-point bending technique [21]. The principle of operation is based on the three-point bending method of a shape memory alloy specimen with known dimensions at different temperatures. The specimens with 10 mm × 0.5 mm × 2.5 mm size were used to study the hysteresis curves of bending strain vs temperature and stress. The measurements were carried out in the temperature range from room temperature to 500 K.

3 Results and Discussion

3.1 Magnetic Properties

The results of studying the magnetic transformation for the Ni_{2.30}Mn_{0.73}Ga_{0.90}Si_{0.07} Heusler alloy in the as-cast and

forged states by recording the magnetization curves are shown in Fig. 2. It is seen that the $M(T)$ curves for the as-cast and thermally treated states have a similar trend. In the magnetic field strength range of 10–30 kOe with increasing temperatures, a monotonic decrease in magnetization is observed. It is characteristic of the transition from the ferromagnetic to paramagnetic phase. In this case, with an increase in the external magnetic field, the phase transformation temperature is shifted to the region of higher temperatures. The temperature is shifted from 370 to 400 K. This behavior is typical of the Ni–Mn–Ga alloys, since the magnetic moment of the manganese atoms is several Bohr magnetons. This increases the interaction energy of the external magnetic field with the magnetic moments of the atoms and maintains ferromagnetic ordering up to higher temperatures. When the magnetic field strength is 0.01 Oe for the as-cast state and 0.05 Oe for the forged state, the measurements show that the Curie temperature is approximately 340 K. Thus, an analysis of the magnetic properties of the Ni_{2.30}Mn_{0.73}Ga_{0.90}Si_{0.07} alloy in both states shows that forging at 973 K and the true strain (ϵ) of 3.9 does not affect the magnetic properties of the alloy.

3.2 Differential Scanning Calorimetry

A precise analysis of the effect of thermomechanical treatment on the temperature of martensitic transformation studied using differential scanning calorimetry is presented in Fig. 3. In the as-cast state, the characteristic temperatures of the phase transformation have the following values: $M_S = 513$ K; $M_F = 427$ K; $A_S = 458$ K; $A_F = 558$ K. The hysteresis of the phase transformation is about 45 K ($A_F - M_S$) and 31 K ($A_S - M_F$). The phase transformation range occupies a temperature range of 131 K ($A_F - M_F$). In the thermally treated state, the transformation characteristic temperatures are shifted to lower temperatures. In this case, the temperatures have the following values: $M_S = 474$ K; $M_F = 411$ K; $A_S = 420$ K; $A_F = 495$ K. The reduction can be estimated from the average value of the direct martensitic transformation ($T_M = (M_S + M_F)/2$). For the as-cast and forged states, these values are 470 K and 442 K, respectively. Thus, the decrease in the martensitic transformation temperature is 28 K. For forged state, the hysteresis has a value of about 21 K ($A_F - M_S$) and 9 K ($A_S - M_F$), which are much lower than those for the as-cast state. The narrowing of the martensitic transformation hysteresis is due to the long-range fields of internal stresses in the specimen. This contributes to the fact that the nucleation and growth of martensitic twins affect the entire volume of the specimen. The decreasing martensitic transformation temperature is due to the restricted movement of the dislocations in the deformed structure. Thus, the TMT makes

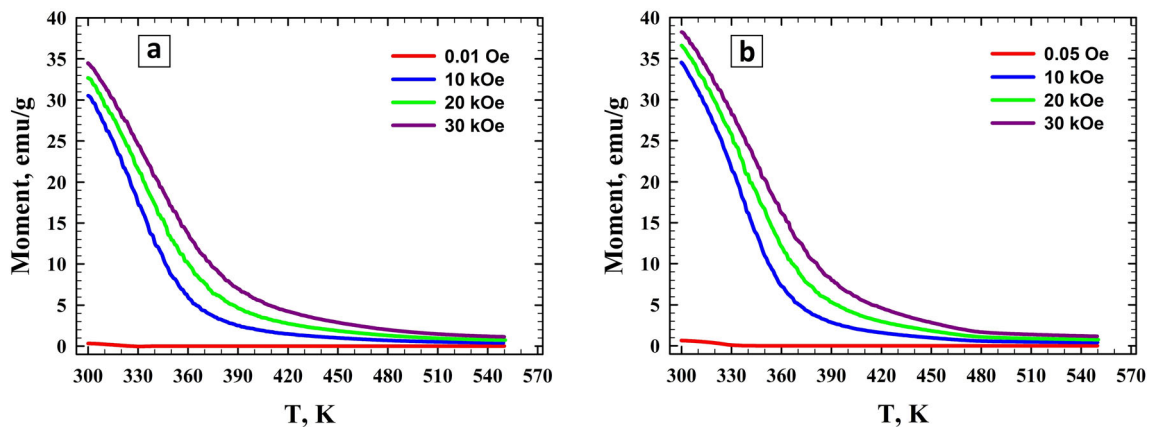


Fig. 2 Magnetization curves of $\text{Ni}_{2.30}\text{Mn}_{0.73}\text{Ga}_{0.90}\text{Si}_{0.07}$ Heusler alloy in the as-cast (a) and forged (b) states in the magnetic field range 0.01–30 kOe

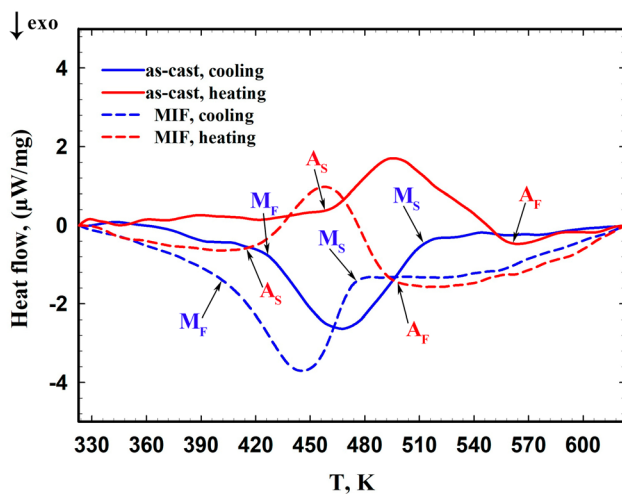


Fig. 3 DSC curves for the $\text{Ni}_{2.30}\text{Mn}_{0.73}\text{Ga}_{0.90}\text{Si}_{0.07}$ Heusler alloy in the as-cast and forged states

it possible to obtain a material with a narrower interval of phase transformation, which in turn should help to reduce the magnetic field strength required to convert the alloy from one phase to another. This will provide significant magnetostrains in lower magnetic fields.

3.3 Microstructure of Alloy in Different States

The microstructure of the as-cast alloy is investigated along a section parallel to the XOY plane (Fig. 1a). This section does not reveal pores and microcracks, which are usually observed after argon-arc melting (Fig. 4). In the as-cast state, the structure consists of the martensite plate colonies with a thickness of several micrometers, formed in the austenite grains upon cooling by shear mechanism. The size and orientation of martensitic colonies are sufficiently isotropic throughout the section, which indicates that during fabrication of the alloy, the crystallographic and

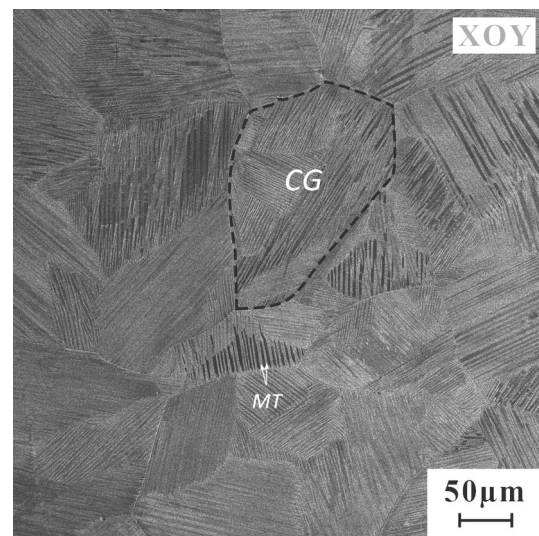


Fig. 4 Microstructure of the $\text{Ni}_{2.30}\text{Mn}_{0.73}\text{Ga}_{0.90}\text{Si}_{0.07}$ Heusler alloy in the as-cast state (CG—coarse grain, MT—martensitic twins)

metallographic textures, a predominant orientation of internal stresses is not formed. The absence of a preferred orientation of the martensitic plates is an important factor that must be taken into account when analyzing the thermal expansion of the alloy during martensitic transformation. Martensitic colonies are observed practically throughout the volume of the alloy, which indicates that the martensitic transformation is complete above room temperature. It is correlated with the DSC data. The austenite grain size, corresponding to the size of martensitic colonies, is about 100–200 μm . Thus, during crystallization of the alloy after additional vacuum-induction remelting, an isotropic structure consisting of relatively equiaxed grains is formed.

The structure of the thermally treated state is analyzed in two sections. These are normal (XOY) and parallel (XOZ) to the drawing axis (Fig. 1b). The image of microstructure across the drawing axis is shown in Fig. 5a. The OY axis,

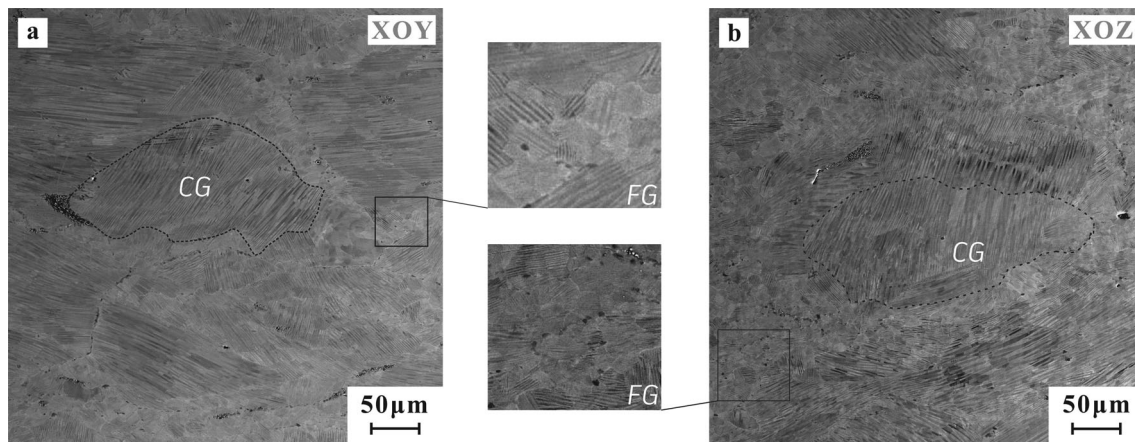


Fig. 5 Microstructure of the forged state in the plane across (a) and along the drawing axis (b) for the $\text{Ni}_{2.30}\text{Mn}_{0.73}\text{Ga}_{0.90}\text{Si}_{0.07}$ Heusler alloy (CG—coarse grain, FG—fine grains)

which is parallel to the final upset, is positioned vertical to the image plane. After forging, a two-phase microstructure is formed in the alloy, in which there are relatively equiaxed coarse grains (CG) of about $100\ \mu\text{m}$, surrounded by fine-grained (FG) structure. Such structure is formed due to the dynamic recrystallization processes at the heat treatment. During the multi-axial isothermal forging, the deformation of the neighboring grains proceeds non-uniformly. Due to the fact that the grains have an arbitrary orientation, it results in the formation of a dislocation density gradient on both sides of the grain boundary. As a result, upon thermal treatment, the threshold deformation is more rapidly achieved in a grain with a higher density of dislocations. It is necessary to activate the processes of nucleation and growth of new grains. As a rule, in the near-boundary regions in a grain with an increased density of dislocations, local migration of individual sections of the high-angle boundary and the formation of relief on it begin. The resulting “reliefs” or “tongues” during further deformation serve as the nuclei for new grains in the sample. The predominant formation of recrystallization nuclei along the boundaries of the initial grains and their growth leads to the appearance of recrystallized regions near these boundaries in the form of finer-grained structure, that is, a “necklace”-type structure is formed. The formation of this type is characteristic of recrystallization processes proceeds by the mechanism of intermittent dynamic recrystallization. The fine-grained structure thickness is about several tens of microns and includes less than 10 grains. In general, the structure throughout the volume of the sample is homogeneous. But in the central part, the thickness is larger than in the periphery. It is due to the fact that during upsetting, the central part of the sample undergoes more intense deformation as compared to the periphery. The body of both large and small grains consists of martensite plate colonies. In this case, the visually

estimated preferential orientation of the martensitic plates is not revealed.

A study of the microstructure along a section parallel to the drawing axis does not reveal significant differences. Despite the elongation of the sample during drawing, the elongated grains along the drawing axis can not be found. In this case, there is also no nucleation of martensitic plates with any preferred orientation. Thus, the metallographic texture of grains and colonies of martensitic plates in the $\text{Ni}_{2.30}\text{Mn}_{0.73}\text{Ga}_{0.90}\text{Si}_{0.07}$ Heusler alloy after forging and drawing in 6 stages has not been established.

3.4 Thermal Expansion of Alloy in As-cast and Thermally Treated States

An analysis of the thermal expansion of the alloy in the as-cast state was performed on a specimen cut across the radius of a cylindrical sample. In Fig. 6, the results of dI/I

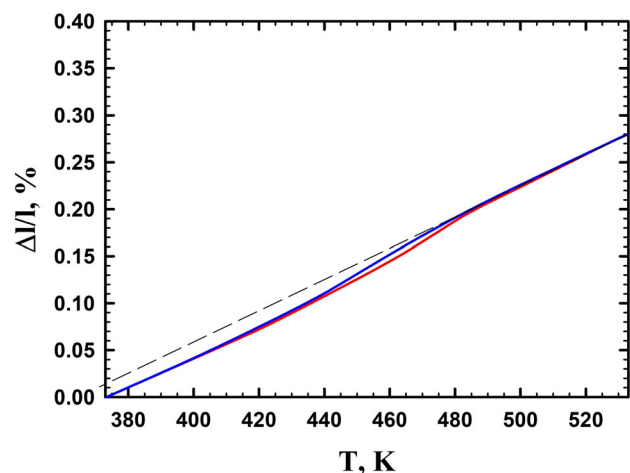


Fig. 6 Thermal expansion of the $\text{Ni}_{2.30}\text{Mn}_{0.73}\text{Ga}_{0.90}\text{Si}_{0.07}$ Heusler alloy in the as-cast state

$l(T)$ upon heating and cooling of the specimen in the 373 K–533 K temperature range are shown. It can be seen that in the range of approximately 433 K–483 K, there is a certain nonmonotonicity and deviation from the anharmonic law. This range corresponds to the martensitic transformation. During the direct martensitic transformation, the specimen undergoes a slight abrupt reduction of length. In order to estimate the contribution of the phase transformation to the change in length, a tangent line is drawn on the graph. The line is parallel to the monotonic change of the specimen length in the austenitic state. Its intersection with the ordinate shows the value of the contribution. In this case, it is very small and amounts to about 0.01%. This indicates that in the process of direct martensitic transformation, a twinned microstructure with an almost chaotic distribution of the martensitic plate orientation is formed. Due to the weak jump-like change of the length, it is difficult to accurately estimate the characteristic temperatures of the phase transformation.

To analyze the anisotropy of the forged state, specimens were cut in two perpendicular directions. These are along the treatment axis (drawing axis, OZ), and in the direction of the final upsetting (OY). For OZ direction, the results are presented in Fig. 7a. In the process of direct martensitic transformation, the specimen elongates abruptly, while in the opposite case, it contracts. Let us designate this behavior as “up jump.” In this case, the contribution of the martensitic transformation to the specific change of dimensions is about 0.08%. It can be seen from the heating and cooling curves that the characteristic temperatures of the martensitic transformation have the following values: $M_S = 455$ K; $M_F = 390$ K; $A_S = 425$ K; $A_F = 475$ K.

The thermal expansion of a specimen cut across the drawing axis and along the direction of the final upsetting demonstrates that “up jump” is replaced by the “down jump” (Fig. 7b). In this case, the contribution of the martensitic transformation is 0.15%. In this specimen, the

temperatures of phase transformation are $M_S = 465$ K; $M_F = 410$ K; $A_S = 430$ K; $A_F = 475$ K. The characteristic temperatures of the phase transformation determined by the dilatometry method differ from the DSC data due to the absence of direct contact of the thermocouple with the specimen in the dilatometry method. This can also be confirmed by the less sharp inflections on the $dl/l(T)$ curves. Thus, forging of the alloy makes it possible to form a certain preferential orientation of internal stresses in the material which lead to anisotropy of thermal expansion in the martensitic transformation region. In this case, the abrupt changes of the length are characteristic of the Ni–Mn–Ga Heusler alloys in the as-cast state. This should have a positive effect on the magnetically induced strains of the alloy.

3.5 Shape Memory Effect and Stability of Martensitic Transformation

The dependence of the bending deformation on temperature and the number of thermal cycles is studied only for the forged state. The thermal cycling study of the reversible deformation takes a long time (days or weeks, depending on the magnitude of stresses relative to the conventional yield stress). At the same time, tests are carried out adhering to a soft cycle, i.e., by fixing the applied strains. Therefore, we have compared the forged state of the studied alloy ($\text{Ni}_{2.30}\text{Mn}_{0.73}\text{Ga}_{0.90}\text{Si}_{0.07}$) and the as-cast state of a similar $\text{Ni}_{2.16}\text{Mn}_{0.78}\text{Ga}_{0.98}\text{Si}_{0.07}$ alloy published in [22].

Initially, to determine the level of applied stresses during cyclic tests, a study of thermomechanical properties is carried out under various forces, which introduce permanent stresses in the specimen. In each new thermal cycle (heating–cooling–heating), the value of the applied force increases and then again, the specimen passes the next thermal cycle and so on until the specimen breaks. Such

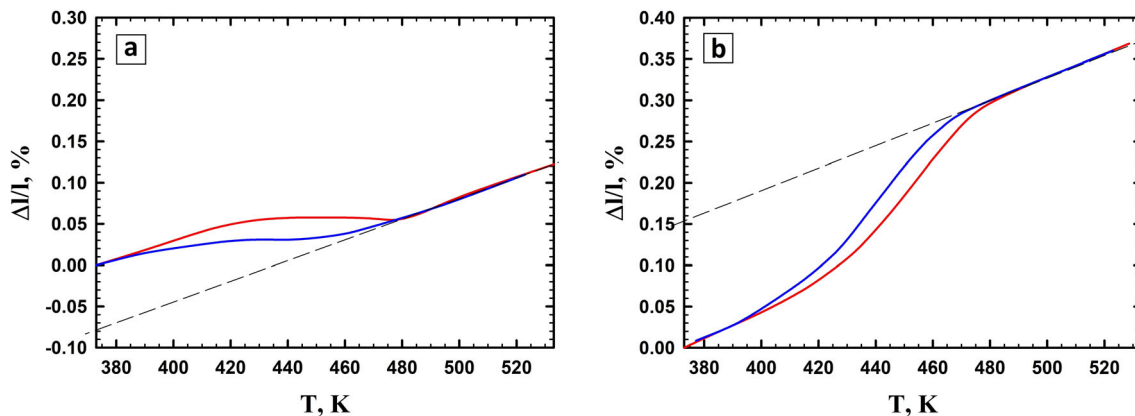


Fig. 7 Thermal expansion of the forged alloy along (OZ) and across (OY) of the drawing for $\text{Ni}_{2.30}\text{Mn}_{0.73}\text{Ga}_{0.90}\text{Si}_{0.07}$ Heusler alloy

curves of the thermoelastic transformation hysteresis make it possible to determine the reversible deformation value during the form recovery under stress and both the phase transformations temperatures and their displacement under the influence of stresses. In Fig. 8, the results of three-point bend tests are shown, indicating the dependence of the bending strain of the specimen (ϵ) on temperature (t) and stress (σ).

The difference in the chemical composition of the forged and the previously studied as-cast alloys leads to a difference in the temperatures of phase transformation. It can be seen that the forged state significantly supersedes the as-cast state both in terms of reversible deformation (ϵ_r^σ) and stresses (σ), at which the specimen breaks showing the greatest ϵ_r^σ value. Thus, for the forged state, the maximum ϵ_r^σ value is 3.1% ($\epsilon_r^{860} = 3.1\%$) at a stress of 860 MPa (σ_{cr} is the critical stress, above which an intense accumulation of plastic deformation begins and a decrease in reversible deformation occurs) and for the cast state $\epsilon_r^{380} = 1.5\%$.

In Fig. 9, the stress dependence of reversible deformation and phase transformation temperature is shown. It should be noted that the applied stresses have no significant effect on the phase transformation temperatures for the Heusler alloys (blue and red curves on the figure). The increment interval, Δt , which is calculated as the difference between A_F and M_F , is 323 K at low stresses (up to 360 MPa) and increases to 358 K at stress of 860 MPa. The enlargement of the phase transformation interval is due to an increase in the level of internal stresses for the material with an increase in stress. At the above strains (up to 860 MPa), the deformation of the specimen is carried out in the elastic region. An increase in internal stress values leads to an increase in the potential barrier for both the direct martensitic transformation and the reverse

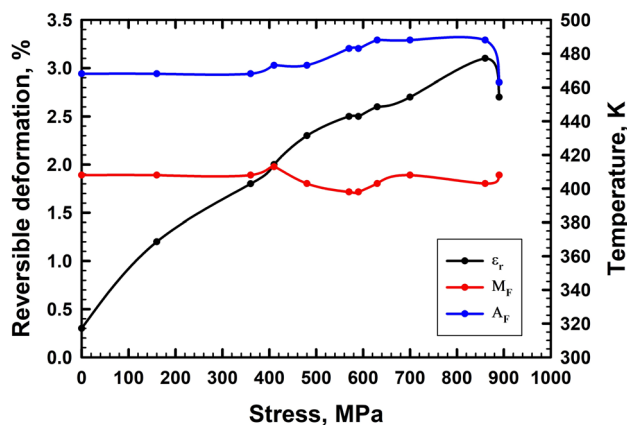


Fig. 9 Dependence of the of reversible deformation and the A_F and M_F temperatures on stress for $Ni_{2.30}Mn_{0.73}Ga_{0.90}Si_{0.07}$ Heusler alloy (forged state)

transformation. To overcome this barrier, additional energy or a greater change of the system temperature is needed.

As published in an earlier work [22], for alloys showing brittle fracture (Heusler alloys), functional fatigue begins to decrease at stresses of $0.5\sigma_{cr}$, which in this case is about 430 MPa. Thus, cyclic tests were carried out at stresses above 430 MPa. The dependence of reversible deformation on the number of thermal cycles is most interesting. Figure 10 shows the above tendencies for the forged and as-cast states [22]. It should be noted that at relatively lower stresses, the behavior of the specimens is characterized by an increase in the reversible deformation and an increase in the number of thermal cycles. Thus, for a forged specimen at a stress of 550 MPa, the reversible deformation is initially at 4.5% and then increases to 5%. (For the as-cast specimen at 100 MPa, it increases from 0.5 to 1.5%). At this stress level, the specimen can withstand about 1500 cycles without destruction. When the stress increases to 650 MPa, the reversible deformation decreases from 5.5% to 4.5%, and then, brittle fracture of the

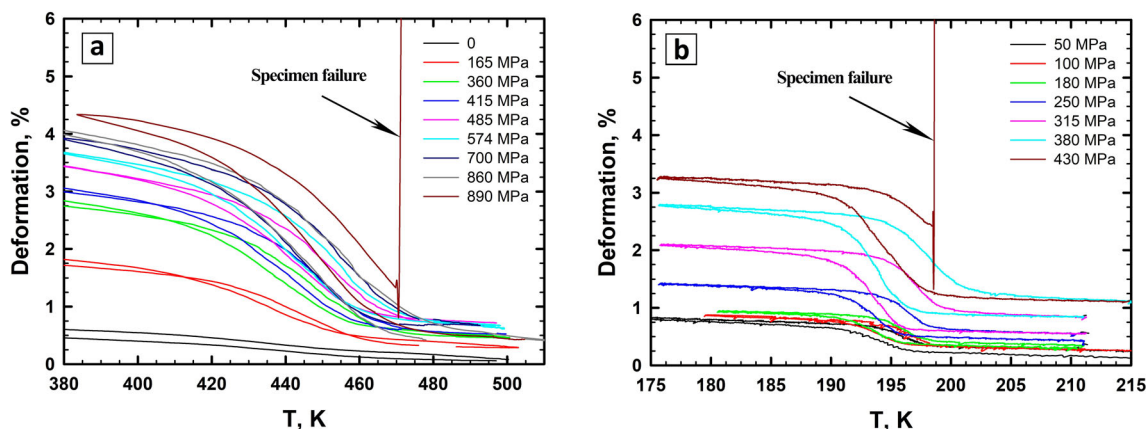


Fig. 8 Dependence of ϵ on strain and temperature for the forged state ($Ni_{2.30}Mn_{0.73}Ga_{0.90}Si_{0.07}$) (a) and for as-cast state ($Ni_{2.16}Mn_{0.78}Ga_{0.98}Si_{0.07}$) (b) [22]

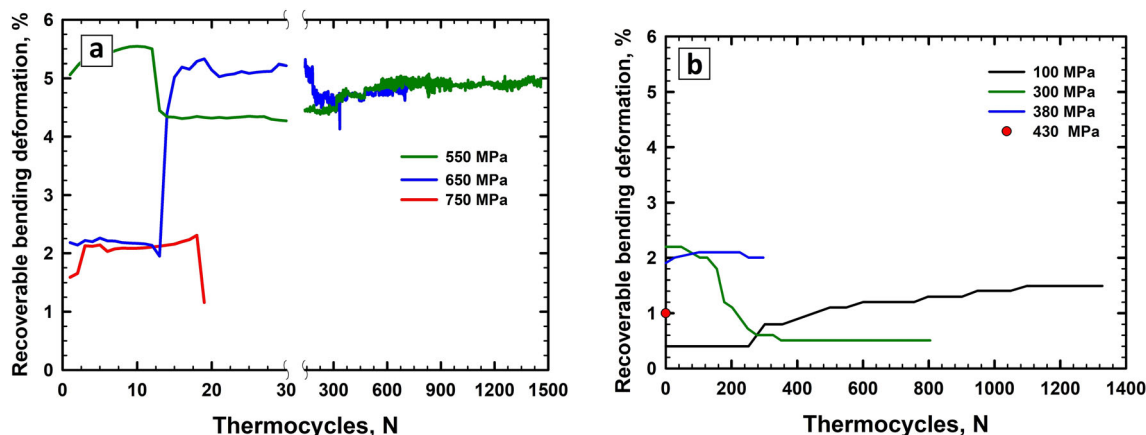


Fig. 10 Dependence of the reversible deformation on the thermal cycles for the forged state (Ni_{2.30}Mn_{0.73}Ga_{0.90}Si_{0.07}) (a) and for the as-cast state (Ni_{2.16}Mn_{0.78}Ga_{0.98}Si_{0.07}) (b) [22]

specimen occurs after 711 cycles (A gradual decrease in reversible deformation is not observed; the crack is formed during the phase transformation and rapidly develops over the cross section of the specimen.). For the as-cast state at 300 MPa, the reversible deformation decreases from 2.1% to 0.5% and the specimen is destroyed at cycle 800. When the stress is increased to 750 MPa, the reversible deformation decreases to 2%, and then, at the twentieth cycle the brittle fracture of the specimen occurs. Significant differences are therefore observed at relatively high stresses, as the forged sample exhibits relatively low values of reversible deformation in the beginning and then it decreases rapidly. On the contrary, the as-cast specimen shows high values of reversible deformation in the beginning and then it decreases.

The results obtained from thermocycling experiments show how the material resists the accumulation of plastic deformation and also indicate a strong instability of thermomechanical properties, which are most likely associated with its processing technology. The authors propose to decrease the forging temperature during the final steps of heat treatment. It increases the level of the internal stresses, which should increase the reversible deformation. Nevertheless, the forged state demonstrates significantly higher thermomechanical and fatigue characteristics. The critical stresses are approximately 1.5–2 times higher for functional fatigue and 5 times higher for reversible deformation. The microstructural parameters (i.e., the difference between the forged and as-cast states) does not affect the accumulation of plastic deformation during cycling in general. Almost, a certain average stress between $0.5\sigma_{cr}$ and σ_{cr} , the accumulation of plastic deformation follows the same trend (Fig. 10 for the dependence of reversible deformation on the number of thermal cycles at 650 MPa for forged specimen, at 300 MPa for the as-cast specimen), i.e., a decrease of reversible deformation is a consequence of an increase of plastic deformation.

4 Conclusions

The analysis of the effect of thermomechanical treatment by the multi-axial forging at 973 K and true strain (ϵ) of 3.9 on the microstructure, magnetic, dilatometric and mechanical properties of the Ni_{2.30}Mn_{0.73}Ga_{0.90}Si_{0.07} alloy leads to the following conclusions:

- As a result of thermomechanical treatment, a decrease in the characteristic martensitic transformation temperatures to the low temperature region (~ 28 K) is observed. In this case, the hysteresis of the phase transformation is narrowed down by about two times. It should help reduce the magnetic field strength required to transform the alloy from one phase to another. In turn, this will provide significant magnetostrains in lower magnetic fields.
- Forging of the alloy results in the formation of a two-phase microstructure. The initial large grains of about 100 μm are surrounded by a fine-grained structure with several tens of micron thickness. This type of microstructure should increase the mechanical properties of alloy because the interlayer will serve as a sink of internal stresses during the martensitic transformation. The presence of metallographic and martensitic twin textures after forging and drawing has not been established.
- In the martensitic transformation range for the as-cast state, the isotropic behavior of the specimen is replaced by the anisotropy of thermal expansion in the heat-treated state. The specimen cut in the direction of the drawing axis during the direct martensitic transformation is elongated by 0.08%. But the specimen cut across the drawing axis and along the direction of the final upsetting is compressed by 0.15%. As per the literature, such anisotropic strain values are quite close to those of the alloys in the as-cast state. Thus, with the help of

TMT by MIF, it is possible to form anisotropic properties in the as-cast state.

- A study of the thermomechanical properties shows that the specimen demonstrates a reversible strain of 3.1% at 860 MPa ($0.5\sigma_{cr}$), and a reversible strain of 4.5–5% during cyclic tests at 550 MPa, having more than 4000 thermal cycles without failure. The increase in stress does not strongly affect the phase transformation temperatures.
- A study of the dependence of reversible deformation on the number of thermal cycles shows that the nature of the plastic deformation accumulation (as a consequence of the decreases in reversible strain) is similar to that studied earlier for the as-cast state. During thermal cycling, the embrittlement process occurs in the range between $0.5\sigma_{cr}$ and $0.5\sigma_{cr}$.

Thus, thermomechanical treatment by the multi-axial isothermal forging at 973 K and true strain (ϵ) of 3.9 significantly increases the operational properties in comparison with those for the as-cast state. However, the value of the thermal expansion anisotropy in the martensitic transformation region is still not large enough and less than that observed for Ni-Mn-Ga alloys. The anisotropy must be increased in order to increase the value of the magnetically induced strain. To achieve this, it is necessary to increase the level of internal stresses in the material by lowering the treatment temperature.

Acknowledgements The investigation of the microstructure, influence of forging on the temperature of martensitic transformation, anisotropy of the thermal expansion, value of the reversible strain and thermal cycle stability was accomplished as per the State assignment of the IMSP RAS (for M.I.I., S.I.M., G.R.M., G.R.Y., A.D.D.). The investigation of the magnetic properties was accomplished according to the State assignment of the IRE RAS (for D.E.T., K.V.S., K.V.V.). And also, one of the authors (D.E.T.) gratefully acknowledges partial support by President of Russian Federation (Grant No. MK-355.2020.2).

The deformation processing and microstructure studies were carried out using the facilities of shared services center of the Institute for Metals Superplasticity Problems of Russian Academy of Sciences “Structural and Physical-Mechanical Studies of Materials.”

Declaration

Conflicts of interest The authors declare that they have no conflict of interest.

References

- [1] Pagounis E, Chulist R, Szczerba M J, Laufenberg M, *Appl. Phys. Lett.* **105**(5) (2014) 052405.
- [2] Pagounis E, Szczerba M J, Chulist R, Laufenberg M, *Appl. Phys. Lett.* **107**(15) (2015) 152407.
- [3] Sozinov A, Lanska N, Soroka A, Zou W, *Appl. Phys. Lett.* **102**(2) (2013) 021902.
- [4] Zhou Z, Wu P, Ma G, Yang B, Li Z, Zhou T, Wang D, Du Y, *J. Alloys Compd.* **792** (2019) 399.
- [5] Gaitzsch U, Potschke M, Roth S, Rellinghaus B, Schultz L, *Acta Mater.* **57**(2) (2009) 365.
- [6] Mendonca A A, Jurado J F, Stuard S J, Silva L E L, Eslava G G, Cohen L F, Ghivelder L, Gomes A M, *J. Alloys Compd.* **738** (2018) 509.
- [7] Everhart W, Newkirk J, *Heliyon* **5**(5) (2019) e01578.
- [8] Aliev A M, Batdalov A B, Khanov L N, Mashirov A V, Dilmieva E T, Koledov V V, Shavrov V G, *Phys. Solid State* **62**(5) (2020) 837.
- [9] Chulist R, Bohm A, Rybacki E, Lippmann T, Oertel C-G, Skrotzki W, *Mater. Sci. Forum* **702–703** (2012) 169.
- [10] Kaletina Y V, Greshnova E D, Kaletin A Y, Frolova N Y, Pilyugin V P, *Phys. Met. Metallogr.* **120**(2) (2019) 171.
- [11] Pushin V G, Kuranova N N, Marchenkova E B, Pushin A V, *Phys. Met. Metallogr.* **121**(4) (2020) 330.
- [12] Pushin V G, Kuranova N N, Marchenkova E B, Pushin A V, *Tech. Phys.* **65**(4) (2020) 602.
- [13] Morawiec H, Goryczka T, Drdzen A, Lelatko J, Prusik K, *Solid State Phenom.* **154** (2009) 133.
- [14] Musabirov I I, Safarov I M, Galeyev R M, Gaisin R A, Koledov V V, Mulyukov R R, *Phys. Solid State* **60**(6) (2018) 1061.
- [15] Wei L, Zhang X, Qiana M, Cui X, Geng L, Sun J, Panina L V, Peng H-X, *Mater. Des.* **112** (2016) 339.
- [16] Chulist R, Skrotzki W, Oertel C G, Bohm A, Brokmeier H G, Lippmann T, *Int. J. Mater. Res.* **103**(5) (2012) 575.
- [17] Musabirov I I, Safarov I M, Galeyev R M, Abdullina D R, Koledov V V, Mulyukov R R, *IOP Conference Series: Materials Science and Engineering.* **447** (2018) 012024.
- [18] Musabirov I I, Safarov I M, Galeyev R M, Abdullina D R, Gaifullin R Y, Afonichev D D, Koledov V V, Mulyukov R R, *Materials Physics and Mechanics.* **40**(2) (2018) 201.
- [19] Musabirov I I, Galeyev R M, Safarov I M, *J. Magn. Magn. Mater.* **514** (2020) 167160.
- [20] Wei L, Zhang X, Gan W, Ding C, Geng L, *Scr. Mater.* **168** (2019) 28.
- [21] Kalashnikov V S, Koledov V V, Kuchin D S, Petrov A V, Shavrov V G, *Instrum. Exp. Tech.* **61**(2) (2018) 306.
- [22] Kalashnikov V S, Koledov V V, Shavrov V G, Musabirov I I, Andreev V A, Gunderov D V, *Tech. Phys.* **65**(4) (2020) 578.

Publisher’s Note Springer Nature remains neutral with regard to jurisdictional claims in published maps and institutional affiliations.